Human kidney-derived tubular organoid, tubuloid, recapitulates cellular senescence, inflammation and fibrosis by repeated-cisplatin treatment

Yuki Nakao[1#], Yutaro Mori[1#*], Makiko Mori[1], Shintaro Mandai[1], Tamami Fujiki[1], Hiroaki Kikuchi[1], Fumiaki Ando[1], Koichiro Susa[1], Takayasu Mori[1], Yuma Waseda[2], Soichiro Yoshida[2], Yasuhisa Fujii[2], Eisei Sohara[1], Shinichi Uchida[1]

[1]Department of Nephrology and [2]Department of Urology, Graduate School of Medical and Dental Sciences, Tokyo Medical and Dental University, Tokyo 113-8510, Japan.

[#]These authors contributed equally to this work.

Lead contact and Corresponding author:

Yutaro Mori, MD, PhD

Department of Nephrology

Graduate School of Medical and Dental Sciences

Tokyo Medical and Dental University

1-5-45, Yushima, Bunkyo-ku, Tokyo 113-8510, Japan

Phone: +81-3-5803-5214; Fax: +81-3-5803-5215; Email: y-mori.kid@tmd.ac.jp

Abstract

Kidney organoids derived from human pluripotent stem cells have been an attracting pathophysiological model recapitulating the response of human kidney to drugs in recent years. Here, we have developed an alternative way to make more homogeneous epithelial-like structures called "tubuloid" based on primary human renal proximal tubular epithelial cells (hRPTECs) cultured from human resected kidneys and tested their efficacy by administering cisplatin at three concentrations of 0.2, 2.0, and 20.0 μg/mL. Tubuloids showed highly differentiated structures composed of proximal tubular epithelial cells with expression of LTL and LRP2/Megalin. Treatment of tubuloids with cisplatin increased γH2AX, a marker for DNA damage, in a dose-dependent manner. Kidney Injury Molecule-1 (KIM-1), a marker of kidney injury, and cleaved caspase-3, a marker for apoptotic signals were expressed due to cisplatin treatment. Repeated administration of cisplatin resulted in upregulation of the cellular senescence marker p16 and enhanced expression of inflammatory cytokines IL-1β and IL-6, indicating an induced senescence-associated secretory phenotype (SASP). Myofibroblast activation was also induced by the supernatant collected from cisplatin-treated tubuloids, which could reflect renal fibrosis. Thus, we succeeded in establishing a model of cisplatin-induced kidney injury based on tubuloids using hRPTECs. Tubuloids have the potential to serve as a novel pathological model and can be utilized to simulate the response of renal epithelial cells to toxins and therapeutic agents. Given its capability to replicate cellular senescence, SASP and the fibrosis, tubuloids could potentially serve as a pathophysiological model for chronic kidney disease (CKD), which is known for fibrosis as a final common pathological pathway.

Key words

organoid, cisplatin nephrotoxicity, fibrosis, chronic kidney disease (CKD)

40 **Introduction**

41 Chronic kidney disease (CKD) is an irreversible progressive condition characterized by the
42 eventual sclerosis of glomeruli, and atrophy and collapse of tubules along with the infiltration of
43 inflammatory cells and fibrosis in the interstitial tissue[1]. Currently, CKD has not been fully
44 elucidated in terms of its pathogenic mechanisms, and a definitive cure is yet to be identified.

45 In recent years, a common mechanism underlying inflammation and fibrosis in CKD has
46 been proposed, starting with DNA damage in tubular epithelial cells and progressing through a
47 cascade involving DNA damage response, cell cycle arrest[2], cellular senescence[3, 4], and the
48 emergence of the senescence-associated secretory phenotype (SASP)[5]. Various models,
49 including cell and animal models, as well as kidney organoids derived from human induced
50 pluripotent stem cells (iPSCs)[6] or human embryonic stem cells (ESCs), have been developed to
51 mimic CKD pathology[7]. However, these models lack the incorporation of the aging process,
52 particularly cellular senescence, observed in humans with a lifespan exceeding 80 years.
53 Experimental animals such as mice, with a lifespan of only two years, does not perfectly replicate
54 age-related diseases associated with cellular senescence. Additionally, kidney organoids derived
55 from iPSCs or ESCs have yet to surpass the stage of reproducing fetal kidney development,
56 remaining distant from faithfully recapitulating age-related diseases such as CKD.

57 In this context, "tubuloids", first reported in 2019, are three-dimensional structures
58 resembling renal tubules, established from adult primary human renal proximal tubular epithelial
59 cells (hRPTECs)[8]. Schutgens et al. cultured primary hRPTECs from adult human kidney and
60 urine, and succeeded to produce tubuloids which would recapitulate viral infection to proximal
61 tubules and hereditary diseases[9]. We also developed tubuloids from human resected kidneys by
62 using a more refined protocol[10] and presented response to a nephrotoxicant and a candidate

63 therapeutic agent. The establishment of a pathophysiological model for aging or senescence-
64 associated disease, however, has not progressed yet.

65 Cisplatin is used as a therapeutic agent for various malignancies, including lung cancer. As
66 an adverse effect, cisplatin-induced nephropathy is well known[11, 12], in which DNA damage is
67 induced in renal proximal tubules[13]. DNA damage response by the cells could lead cell cycle
68 arrest during repairing phase after cisplatin-induced injury, followed by cellular senescence and
69 SASP that are the final detrimental mechanisms, which could explain acute kidney injury (AKI)
70 to CKD transition[14, 15]. Thus, to recapitulate cisplatin-induced nephropathy is not only a simple
71 nephrotoxicant disease modeling, but also a potential trial mimicking a pattern of CKD.

72 Here, in this study, we attempted to assess the disease modeling capability by exposing
73 tubuloids to cisplatin, aiming to reproduce cisplatin-induced nephropathy. We also investigated
74 whether we could replicate cellular senescence and associated response beyond cisplatin
75 nephrotoxicity aiming to recapitulate AKI to CKD transition or CKD itself.

76

77 **Results**

78 **Primary human renal proximal tubular epithelial cells (hRPTECs) form highly polarized**
79 **structure**

80 To establish tubuloids, human renal proximal tubular epithelial cells (hRPTECs) were isolated
81 from the human kidney cortex, embedded in a basement membrane gel, and cultured in the
82 presence of various growth factors **(Figure 1A)**. By finely mincing the cortex portion of the human
83 kidney and selectively culturing epithelial cells in a serum-free medium with Epidermal Growth
84 Factor (EGF), primary cultured cells, mainly proximal tubular epithelial cells, were successfully
85 established **(Figure 1B and 1C)**. Subsequently, tubuloids were developed over approximately a

86 two-week protocol **(Figure 1D).** In detail, hRPTECs were seeded on an ultralow attachment plate
87 **(Figure 1E).** Matrigel and media containing fetal bovine serum, EGF, Fibroblast Growth Factor 2
88 (FGF2), and Hepatocyte Growth Factor (HGF). Multiple tubuloids were formed within a single
89 well, displaying the nearly uniform size. The epithelial cells formed tubular-like structures
90 surrounding the basement membrane gel **(Figure 1F)**. By moving the microscope in Z-axis
91 direction, the three-dimensional architecture was confirmed **(Figure 1G)**. The cells formed a
92 monolayer structure resembling tubules or renal cysts, not spheroid-like structure. Tubuloids
93 expressed differentiation markers for proximal tubular epithelial cells, such as lotus tetragonolobus
94 lectin (LTL) and LDL Receptor Related Protein 2 (LRP2/Megalin), indicating that they constituted
95 highly differentiated and polarized structure **(Figure 1H)**[16].
96
97 **Cisplatin-treated tubuloids show collapse of tubular structure and various acute response as**
98 **DNA damage response (DDR)**
99 To assess their reactivity against a nephrotoxicant, tubuloids were exposed to cisplatin. Cisplatin
100 is known to induce renal injury and elicit various physiological responses. Organic Cation
101 Transporter 2 (OCT2) mediates the uptake of cisplatin into proximal tubular epithelial cells[17]
102 and cisplatin causes DNA damage directly **(Figure 2A)**. Upregulation of a DNA damage and
103 response marker, γH2AX, was reported both *in vivo* and *in vitro*[18]. Initially, tubuloids were
104 treated with cisplatin at three concentrations of 0.2, 2.0, and 20.0 μg/mL. The three-dimensional
105 structure of tubuloids was collapsed due to treatment with high-dose cisplatin **(Figure 2B)**, a
106 marker for DNA damage, was increased in a dose-dependent manner **(Figure 2C).** Representing
107 differentiation markers such as LRP2 and Na^+/K^+-ATPase were decreased by cisplatin treatment,
108 indicating that cells are in a dedifferentiation process **(Figure 2D and 2E).**

109 Moreover, an upregulation in the expression of a renal injury marker, Kidney Injury
110 Molecule-1 (KIM-1)[19], and an apoptosis marker, Cleaved Caspase-3, were also noted **(Figure**
111 **2F, G and H)**, which is consistent with previous reports[20]. From these observations, we
112 confirmed that tubuloids exhibit a sensitive response to cisplatin, displaying the acute responses
113 as DNA damage response (DDR).

114 When high concentrations of cisplatin were administered, an increase in the expression of
115 Vimentin, an intermediate filament specific to mesenchymal cells, was observed **(Figure 2I and**
116 **J).** This suggests that proximal tubular epithelial cells may undergo epithelial-mesenchymal
117 transition (EMT) for tissue repair[21, 22]. Vimentin activation after DDR is known[23] and we
118 could also confirm following reaction in this study.

119

120 **Tubuloids show cellular senescence and release inflammatory cytokines, following repeated**
121 **cisplatin treatment**

122 To assess the possibility of reproducing chronic responses in tubuloids, we treated them with
123 cisplatin over an extended period. Initially, cisplatin was administered at concentrations of 0.2 and
124 2.0 μg/mL. Subsequently, the media was changed three times to minimize residual cisplatin,
125 followed by regular culture in standard media for one day. This was considered as one cycle, and
126 the following day, cisplatin was administered again at similar concentrations **(Figure 3A)**. This
127 process was repeated five times. As presented in **Figure 2**, treatment with 20.0 μg/mL cisplatin
128 led to the disruption of tubuloids and cell death strongly. Accordingly, to confirm the long-term
129 chronic response of tubuloids, this concentration was avoided in the experimental setup.

130 In the repeated cisplatin administration model, expression of p16, a marker for cellular
131 senescence, was observed **(Figure 3B, C and D)** as reported previously[24]. Increased expression

132 of the inflammatory cytokine IL-1β was confirmed at 2.0 μg/mL as well by immunofluorescence
133 **(Figure 3D)**. Compared to controls, the group subjected to repeated administration of 2.0 μg/mL
134 cisplatin showed a 50-100-fold increase in mRNA levels of both IL-1β and IL-6 by quantitative
135 PCR **(Figure 3E and F)**. These data suggest that repetitive DNA damage induced by cisplatin led
136 to cellular senescence, resulting in the acquisition of a SASP.
137
138 **Secretion released from cisplatin-treated tubuloids strongly promotes myofibroblast**
139 **differentiation *in vitro***
140 We hypothesized that prolonged exposure of tubuloids to high concentrations of cisplatin might
141 promote myofibroblast activation, potentially leading to tissue fibrosis through the secretion of
142 paracrine factors from tubuloids as well as reported *in vivo*[25]. To test this hypothesis, we
143 performed a fibrosis bioassay based on previous reports[10] **(Figure 4A)**. Initially, tubuloids were
144 divided into three groups: one receiving no cisplatin, one receiving 0.2 μg/mL cisplatin, and
145 another receiving 2.0 μg/mL cisplatin. Each group was treated repeatedly. After cisplatin
146 administrations, the medium was changed three times, and cisplatin was removed. The tubuloids
147 were then left for 2 days in a serum-free condition to obtain conditioned media (CM) containing
148 secreted paracrine factors. The collected CM were subsequently administered to fibroblasts
149 established from mouse renal cortex **(Figure 4B)**, and myofibroblast activation was evaluated
150 using α-smooth muscle actin (α-SMA)[26]. We observed that CM obtained from tubuloids
151 repeatedly treated with 2.0 μg/mL cisplatin promoted fibrosis most significantly **(Figure 4C and**
152 **D).** This concentration of cisplatin, as indicated in **Figure 3**, corresponds to the maximal secretion
153 levels of IL-1β and IL-6 from tubuloids, demonstrating consistency. Furthermore, direct
154 administration of cisplatin to mouse fibroblasts did not promote myofibroblast defferentiation at

155 all, decisively ruling out cisplatin as a direct fibrosis inducer on fibroblasts. Through the fibrosis
156 bioassay, we confirmed that various paracrine factors secreted from tubuloids with repeated
157 treatment of cisplatin have a fibrogenic effect on tissues.
158
159 **Discussion**
160 In this study, we confirmed that tubuloids experienced DNA damage induced by cisplatin, as
161 evidenced by a dose-dependent increase in γH2AX expression. In response to DNA damage,
162 tubuloids demonstrate a sensitive acute phase response, leading to elevated expression of the
163 kidney injury marker, KIM-1, and the apoptosis marker, Cleaved Caspase-3, according to DDR.
164 As a following reaction, Vimentin expression which is representing EMT was also observed. The
165 well-maintained three-dimensional structure of tubuloids collapsed upon exposure to cisplatin,
166 accompanied by dedifferentiation with reduced expression levels of Na^+/K^+-ATPase and
167 LRP2/Megalin. Furthermore, repeated long-term administration of cisplatin induced an increase
168 in the expression of the cellular senescence marker, p16. Tubuloids acquired senescence-
169 associated secretory phenotype (SASP) and secreted inflammatory cytokines such as IL-1β and
170 IL-6, thereby eliciting a chronic inflammatory response in the surrounding tissues. Secretions from
171 tubuloids significantly promoted fibrosis in surrounding interstitial area, as verified by fibrosis
172 bioassay **(Figure 5).**
173 Research on chronic kidney disease (CKD) is exceedingly challenging due to the diversity
174 and complexity of its underlying conditions. One of the obstacles for investigating CKD is the lack
175 of a faithful disease model. CKD is known for a disease based on aging and senescence. Currently,
176 the predominant disease models are based on mice, which have a lifespan of approximately two
177 years and represent a highly homogeneous population. Two years for mice do not precisely

178 recapitulate decades for humans in terms of chronic disease progression including CKD. Given
179 the variability in CKD progression among humans based on factors such as gender, race, age, and
180 environment, mouse models do not perfectly mimic human CKD, indicating a significant gap.

181 Recently, kidney organoids derived from induced pluripotent stem cells (iPSCs) or
182 embryonic stem cells (ESCs) have garnered attention as promising disease models[27-29]. With
183 current technology, however, these organoids mainly replicate the fetal kidneys, making it
184 challenging to reproduce CKD with age-related features commonly observed in older
185 individuals[30]. Additionally, from a simplicity standpoint, iPSC-derived kidney organoids
186 require complex differentiation induction procedures and skilled techniques. Human resected
187 kidney-derived primary cultured cells in two-dimensional condition do not fully replicate the
188 cellular polarity and three-dimensional structures inherent to living tissues.

189 Conventional disease models for CKD including mouse models, iPSC/ESC kidney
190 organoids, and two-dimensional primary cultured cells from human kidney do have some
191 difficulties with respect to recapitulating aging, senescence, and simplicity of production. Human
192 kidney-derived tubuloids we have developed overcome almost all the weakness of conventional
193 pathological models for CKD. Tubuloids consist of already aged cells based on the patient from
194 whom the cells were derived. They may have senescence to some extent as indicated in **Figure**
195 **3B, C and D**, the control condition without cisplatin treatment. Tubuloids can be formed in a very
196 simple protocol, not requiring skilled techniques. They are cultured in 24-well plates, and as shown
197 in **Figure 1F**, multiple tubuloids are formed within one well. When sampling tubuloids for western
198 blotting, or qPCR and immunofluorescence, we harvested per every well as one independent
199 condition, resulting in multiple tubuloids being included in one sample. This allows for
200 homogenization of variability among individual tubuloids during sampling.

201 Should we produce tubuloids from multiple different patients, we may also be able to
202 recapitulate individual differences in kidney response to various stimuli. Actually, our protocol to
203 produce tubuloids is so stable that we could produce them from different original patients under
204 the same conditions at one time (manuscript in preparation). These characteristics suggest the
205 potential for becoming a novel candidate with advantages as a renal toxicity screening tool in drug
206 discovery.

207 Tubuloids have highly differentiated three-dimensional structure[31] and recapitulate
208 physiological responses to nephrotoxicants[32, 33]. According to previous reports, highly
209 differentiated tubuloids are known to express various channels and transporters and possess more
210 physiological functions compared to two-dimensional cultured cells[34]. These characteristics can
211 contribute to the heightened sensitivity to cisplatin observed in this study, allowing for the
212 recapitulation of cellular senescence and other responses. Tubuloids may replicate biological
213 responses which were not observed in two-dimensional cultured cells.

214 In this study, we have focused on cisplatin-induced nephropathy. Our long-term vision is
215 to create a faithful pathophysiological model for CKD based on human-kidney derived tubuloids.
216 The mechanism of CKD after cisplatin chemotherapy is largely unknown, but treatment with low-
217 dose cisplatin cause long-term renal pathologies with characteristics of CKD previously
218 reported[35]. Cisplatin-induced nephropathy is caused by cisplatin taken up into proximal tubular
219 epithelial cells via OCT2, which directly damages nuclear DNA. DNA damage triggers multiple
220 DNA damage response (DDR) processes: the DDR causes some cells to die, including apoptosis,
221 while some cells enter the cell cycle to compensate for the dead cells. When DNA damage is strong
222 enough, it causes cell cycle arrest, especially in the G2/M phase[2], and further division becomes
223 impossible, indicating cellular senescence. It has been reported that senescent cells secrete multiple

224 inflammatory and fibrotic cytokines through the SASP mechanism, inducing inflammation and
225 fibrosis in the surrounding area, while being resistant to cell death. This mechanism of cellular
226 senescence and SASP triggered by DNA damage has been reported as one of major mechanisms
227 for renal fibrosis and can be considered as an aspect of the AKI to CKD transition and the
228 pathophysiology of CKD itself, beyond cisplatin-induced nephropathy. In tubuloids, we could
229 observe not only differentiated three-dimensional structure, but also pathophysiological responses
230 to cisplatin, i.e., DDR, collapse of structure, dedifferentiation, cell death, epithelial-mesenchymal
231 transition (EMT), cellular senescence, SASP, and fibrotic changes. Our data suggest that tubuloids
232 could be a potential precise disease model for cisplatin-induced nephropathy which faithfully
233 recapitulate most of pathological mechanisms, aiming to development of complete CKD model.
234 Moving forward, we plan to co-culture tubuloids with other cells such as vascular
235 endothelial cells and fibroblasts and simulate urine flow on microfluidic devices to construct more
236 advanced disease models that closely mimic the *in vivo* environment[36].
237 Thus, we succeeded to develop the most precise disease model for cisplatin-induced
238 nephropathy based on human kidney-derived tubuloids. By using tubuloids as a faithful kidney
239 disease model, our understanding of various kidney diseases will be improved. Given its capability
240 to replicate cellular senescence, SASP and the fibrosis, tubuloids could potentially serve as a
241 pathophysiological model for chronic kidney disease (CKD), which is known for fibrosis as a final
242 common pathological pathway.
243
244

245 **Methods**

246 **Cell culture experiment.** Human kidney samples were obtained from clinically indicated
247 nephrectomy in Tokyo Medical and Dental University Hospital in Tokyo, Japan. The protocol was
248 approved by the Institutional Review Board of the Ethics Committee of Tokyo Medical and Dental
249 University (M2022-005). In detail, human renal proximal tubular epithelial cells (hRPTECs) were
250 obtained from the uninvolved parts of kidneys removed by nephrectomy on the renal cell
251 carcinoma or urinary tract malignancy patients by modifying a previously established protocol[37].
252 Briefly, human renal cortex was minced and digested in a solution of Collagenase type II (1.0
253 mg/mL) (Worthington Biochemical, NJ, USA). The enzyme reaction was terminated with fetal
254 bovine serum (FBS). The samples were resuspended in hRPTECs culture medium (DMEM/F-12
255 (Nacalai Tesque, Kyoto, Japan) with BSA (Nacalai Tesque), Antibiotic-Antimycotic
256 (ThermoFisher Scientific, MA, USA), hydrocortisone (ThermoFisher Scientific, MA, USA), ITS
257 liquid media supplement (Sigma-Aldrich, MO, USA), and human recombinant epidermal growth
258 factor (EGF) (ThermoFisher Scientific, MA, USA). The epithelial cells were cultured for 7 to 10
259 days (human) before being used for experiments.

260 For making mouse primary kidney fibroblasts (MPKFs), mouse kidney was minced and
261 then digested in a solution of Collagenase type II (1.0 mg/mL). The enzyme reaction was
262 terminated with FBS. The samples were resuspended in DMEM with 10% FBS and 5ng/ml FGF-
263 basic (ThermoFisher Scientific) and Antibiotic-Antimycotic. The MPKFs were used after 3-5
264 passages.

265 All the cells were maintained in CO2 incubator (5% CO2) at 37o Celsius.

266

267 **Human Renal Tubuloids.** hRPTECs were seeded on ultra-low attachment plates at a density of
268 5.0×10^5 cells/well with Advanced RPMI 1640 medium (ThermoFisher Scientific) containing 5%
269 FBS. After 2 days incubation, Matrigel (Corning, NY, USA) was added. Next day, media was
270 changed to Advanced RPMI 1640 medium containing 5% FBS, EGF, FGF2 and HGF (tubuloids
271 media). Media was changed once or twice a week. The tubuloids are ready for use after 1-2 weeks.
272
273 **Fibrosis bioassay.** The tubuloids were treated with or without cisplatin repeatedly. After 48 h
274 exposure, the media were changed to serum-free DMEM for conditioning. 48 h later, the culture
275 supernatants were collected as conditioned media. MPKFs were plated uniformly at a density of
276 2.0×10^4 cells/well in a 8-well chamber slide (Nunc Lab-Tek Chamber Slide system)
277 (ThermoFisher Scientific) with 10% FBS-DMEM. Next day, conditioned media harvested from
278 the tubuloids were added to MPKFs and incubated for 48 hours. MPKFs on the 8-well chamber
279 slide were washed 2 times with PBS, and immunostained as below.
280
281 **Immunofluorescence staining.** Tubuloids were fixed with 4% paraformaldehyde (PFA) in PBS,
282 and permeabilized with 0.1% Triton X-100 in PBS. After blocking with 3% BSA in PBS, tubuloids
283 were incubated with primary antibodies for 1 hour. Then washed with PBS, tubuloids were
284 incubated with secondary antibodies for 30 minutes and washed with PBS. Tubuloids were
285 transferred onto glass slides, Prolong Glass Antifade Mountant with NucBlue Stain (ThermoFisher
286 Scientific) was applied, and slides were cover-slipped.
287 As primary antibodies, rabbit anti-LRP2 / Megalin antibody (1:100) (ab236244, Abcam,
288 MA, USA), rabbit anti-γH2AX antibody (1:200) (#9718, Cell Signaling Technology, MA, USA),
289 mouse anti-Na^+/K^+-ATPase antibody (1:200) (05-369, Sigma-Aldrich), mouse anti-KIM-1

290 antibody (1:200) (AF1750, R&D systems, MN, USA), rabbit anti-caspase-3 antibody (1:200)
291 (#9664, Cell Signaling Technology), rabbit anti-Vimentin antibody (1:200) (10366-1-AP,
292 Proteintech, IL, USA), rabbit anti-p16-INK4A polyclonal antibody (1:200) (10883-1-AP,
293 Proteintech) , rabbit anti-IL-1β polyclonal antibody (1:200) (bs-0812R, Bioss, MA, USA) and
294 rabbit anti-αSMA antibody conjugated with Cy3 (1:400) (C6198, Sigma-Aldrich) were used. To
295 stain the brush border of the proximal tubular epithelium, LTL, Biotinylated (B-1325-2, Vector
296 Laboratories, CA, USA) was used instead of primary antibodies (1:200). And then streptavidin,
297 Alexa Fluor 633 conjugate (S21375, ThermoFisher Scientific) was used (1:500).

298 For immunofluorescence staining of fibrosis bioassay, MPKFs on an 8-well chamber slide
299 were washed, then fixed with 4% PFA-PBS, and permeabilized with 0.1% Triton X-100 in PBS.
300 After blocking with 3% BSA, cells were incubated with anti-α-SMA antibody (1:200) for 1 hour,
301 washed with PBS, and mounted as described above.

302 All images were obtained by standard or confocal microscopy (Eclipse Ti2 from Nikon),
303 and as operating system, the NIS-Elements Advanced Research microscope system was used.
304 Quantification of stained area was performed by using ImageJ Fiji
305 (https://imagej.net/software/fiji/downloads).

306

307 **qRT-PCR.** qRT-PCR analysis of human IL-1β, IL-6 and 18S mRNA was performed as previously
308 described using the real time PCR detection system with Thermal Cycler Dice Real Time System
309 Lite TP700 (Takara Bio, Shiga, Japan) and TB green Premix Ex Taq II (Takara Bio, Shiga, Japan)
310 [38]. Total RNA was isolated from frozen kidney tubuloids stored at -80°C by using Sepasol-
311 RNAI Super G (Nacalai Tesque, Kyoto, Japan). cDNA was generated with ReverTra Ace

312 (TOYOBO, Tokyo, Japan) from total RNA[39]. cDNA was amplified using 40 PCR cycles with
313 following conditions: 95ºC for 5 seconds, 60ºC for 30 seconds.
314 As primers, nucleotides of followed sequence were used for qRT-PCR.
315 human 18S.
316 Forward:5'-GCAGAATCCACGCCAGTACAAG-3'
317 Reverse:5'-GCTTGTTGTCCAGACCATTGGC-3'
318 human IL-1β.
319 Forward: 5'- CCACAGACCTTCCAGGAGAATG -3'
320 Reverse: 5'- GTGCAGTTCAGTGATCGTACAGG -3'
321 human IL-6.
322 Forward: 5'- AGACAGCCACTCACCTCTTCAG -3'
323 Reverse: 5'- TTCTGCCAGTGCCTCTTTGCTG -3'
324
325 **Western blot analysis.** The tubuloids were lysed and protein was purified. Bands were visualized
326 by Western Blue (Promega, WI, USA). Rabbit anti–ERK2 (p44/42 MAPK) antibody (9102S, Cell
327 Signaling Technology) (1:200) was used as a loading control. Rabbit anti-p16-INK4A polyclonal
328 antibody (1:200) (Proteintech), mouse anti-KIM-1 antibody (1:200) (R&D systems), rabbit anti-
329 caspase-3 antibody (1:200) (Cell Signaling Technology) and rabbit anti-Vimentin antibody (1:200)
330 (Proteintech) were used as primary antibodies. Densitometry was performed by using Image J Fiji
331 (https://imagej.net/software/fiji/downloads).
332
333 **Quantification and Statistical Analysis**

334 Number of samples assayed in each experiment is indicated in the Figure Legends. One-way
335 ANOVA was used to determine a significant difference between each group. $P < 0.05$ was
336 considered to represent a statistically significant difference. GraphPad Prism from GraphPad
337 Software Inc. (San Diego, CA, USA) was used for all the statistical analyses.
338

339 **Acknowledgement**

340 We would like to thank the study participants who kindly allowed to give us the pieces of their
341 resected kidneys.

342

343 **Funding**

344 This work was supported by Leading Initiative for Excellent Young Researchers (LEADER) from
345 Ministry of Education, Culture, Sports, Science and Technology (to Y.M.), Grant-in-Aid for
346 Research Activity Start-up from Japan Society for the Promotion of Science (to Y.M.), Innovation
347 Idea Contest from Tokyo Medical and Dental University (TMDU) (in 2022 to Y.M. and in 2023
348 to Y.N.), Next Generation Researcher Training Unit from TMDU (to Y.M.) and Priority Research
349 Areas Grant from TMDU (to Y.M.), Research Grant from Uehara Memorial Foundation (to Y.M.),
350 Research Grant (Lifestyle-related diseases) from MSD Life Science Foundation (to Y.M.),
351 Medical Research Grant from Takeda Science Foundation (to Y.M.), and Academic Support from
352 Bayer Yakuhin, Ltd. (to Y.M.).

353

354 **Data availability statements**

355 Further information and requests for resources and reagents should be directed to and will be
356 fulfilled by the Lead Contact, Yutaro Mori (y-mori.kid@tmd.ac.jp).

357

358 **Author contributions**

359 Y.N. and Y.M. performed the experiments, collected and analyzed data, and wrote the manuscript.
360 Y.M. and M.M. established the hRPTECs and S.M. helped the procedure. T.F., H.K., F.A., K.S.,
361 T.M., E.S., and S.U. supported the data analysis. Y.W., S.Y. and Y.F. resected the patients' kidneys

362 as standard treatment for malignant diseases. Y.M. developed experimental strategy, supervised
363 the project, and edited the manuscript. All authors discussed the results and implications and
364 commented on the manuscript.
365
366 **Disclosure**
367 The authors declare that they have no conflicts of interest.
368
369

370 **Figure Legends**

371 **Figure 1. Primary human renal proximal tubular epithelial cells (hRPTECs) form highly**
372 **polarized structure, "tubuloids".**

373 **(A)** Outline of establishing tubuloids from hRPTECs derived from human adult kidney.

374 **(B)** Image of the human resected kidney utilized during the establishment of hRPTECs.

375 **(C)** Representative image of hRPTECs. Scale bar: 50 μm.

376 **(D)** Two-week protocol to establish tubuloids from 2D-cultured hRPTECs.

377 **(E)** Representative image of seeding hRPTECs on ultra-low attachment plate. Scale bar: 25 μm.

378 **(F)** Representative Images of tubuloids in each magnification (×10, ×40). Scale bars: 100 μm, 25
379 μm.

380 **(G)** Representative image of tubuloids in ×40 magnification with several layers of Z axis. Scale
381 bars: 25 μm.

382 **(H)** Immunostaining of makers of renal proximal tubular epithelial cells (LRP2/Megalin and LTL).
383 Scale bars: 25 μm.

384

385 **Figure 2. Cisplatin-treated tubuloids show collapse of tubular structure, DNA damage**
386 **response, loss of differentiation, cell death and epithelial-mesenchymal transition.**

387 **(A)** Schematic diagram illustrating the pathway by which cisplatin induces DNA damage in
388 proximal tubular epithelial cells.

389 **(B)** Representative images of tubuloids exposed to cisplatin (0.2, 2.0, 20.0 μg/mL) or control.

390 **(C)** Immunostaining of marker for DNA damage (γH2AX) in tubuloids exposed to cisplatin (0.2,
391 2.0, 20.0 μg/mL) or control. Scale bars: 100 μm.

392 **(D)** Immunostaining of a differentiation marker for epithelial cells, LRP2/Megalin in tubuloids
393 exposed to cisplatin (20.0 μg/mL) or control. Scale bars: 25 μm.
394 **(E)** Immunostaining of a differentiation marker for epithelial cells, Na^+/K^+-ATPase in tubuloids
395 exposed to cisplatin (20.0 μg/mL) or control. Scale bars: 25 μm**.**
396 **(F)** Immunostaining of an epithelial injury marker, Kidney Injury Molecule-1 (KIM-1) in tubuloids
397 exposed to cisplatin (20.0 μg/mL) or control. Scale bars: 25 μm.
398 **(G)** Western blotting of KIM-1 in tubuloids exposed to cisplatin (0.2, 2.0 μg/mL) or control.
399 **(H)** Immunostaining of an apoptosis marker, Cleaved Caspase-3, in tubuloids exposed to cisplatin
400 (20.0 μg/mL) or control. Scale bars: 25 μm.
401 **(I)** Immunostaining of intermediate filament, Vimentin, in tubuloids exposed to cisplatin (20.0
402 μg/mL) or control. Scale bars: 100 μm.
403 **(J)** Western blotting of Vimentin in tubuloids exposed to cisplatin (0.2, 2.0 μg/mL) or control.
404
405 **Figure.3 Tubuloids show cellular senescence and release inflammatory cytokines following**
406 **repeated cisplatin treatment.**
407 **(A)** Experimental design for repeated cisplatin injury.
408 **(B)** Western blotting of p16 in tubuloids exposed to cisplatin (0.2, 2.0 μg/mL) repeatedly or control.
409 **(C)** Quantification of relative protein levels of p16 / ERK1/2. $*P = 0.0233$ ($n = 4$).
410 **(D)** Immunostaining of p16 in tubuloids exposed to cisplatin (2.0 μg/mL) repeatedly or control.
411 Scale bars: 100 μm.
412 **(E)** Immunostaining of an inflammatory cytokine, IL-1β, in tubuloids exposed to cisplatin (2.0
413 μg/mL) repeatedly or control. Scale bars: 100 μm.

414 **(F)** Quantitative PCR of IL-1β and IL-6 in tubuloids exposed to cisplatin (0.2, 2.0 μg/mL)
415 repeatedly or control. Statical analysis was applied to delta-delta Ct value, not fold increase. *P =
416 0.0167 (n = 3), **P = 0.0011 (n = 3).
417
418 **Figure 4. Secretion released from cisplatin-treated tubuloids strongly promotes fibrosis *in*
419 *vitro*.**
420 **(A)** Experimental design for fibrosis bioassay.
421 **(B)** A representative image of Mouse Primary Kidney Fibroblasts (MPKFs). Scale bar: 25 μm.
422 **(C)** Representative images of fibrosis bioassay on MPKFs cultured with Conditioned Media (CM)
423 harvested from tubuloids exposed to cisplatin (0.2, 2.0 μg/mL) or control, or directly with
424 cisplatin-containing media. Scale bars: 100 μm.
425 **(D)** Quantification of αSMA-positive area in MPKFs cultured with CM or directly with cisplatin-
426 containing media measured by Image J. **P = 0.0021, ***P = 0.0001, ****P < 0.0001. (n = 8-10
427 each condition)

428 **References**

429 1. Humphreys, B.D., *Mechanisms of Renal Fibrosis.* Annu Rev Physiol, 2018. **80**: p. 309-326.
430 2. Yang, L., et al., *Epithelial cell cycle arrest in G2/M mediates kidney fibrosis after injury.*
431 Nat Med, 2010. **16**(5): p. 535-43, 1p following 143.
432 3. Sturmlechner, I., et al., *Cellular senescence in renal ageing and disease.* Nat Rev Nephrol,
433 2017. **13**(2): p. 77-89.
434 4. Docherty, M.H., et al., *Cellular Senescence in the Kidney.* J Am Soc Nephrol, 2019. **30**(5):
435 p. 726-736.
436 5. Mylonas, K.J., et al., *Cellular senescence inhibits renal regeneration after injury in mice,*
437 *with senolytic treatment promoting repair.* Sci Transl Med, 2021. **13**(594).
438 6. Takasato, M., et al., *Kidney organoids from human iPS cells contain multiple lineages and*
439 *model human nephrogenesis.* Nature, 2015. **526**(7574): p. 564-8.
440 7. Liu, M., et al., *Studying Kidney Diseases Using Organoid Models.* Front Cell Dev Biol,
441 2022. **10**: p. 845401.
442 8. Schutgens, F., et al., *Tubuloids derived from human adult kidney and urine for personalized*
443 *disease modeling.* Nat Biotechnol, 2019. **37**(3): p. 303-313.
444 9. Xu, Y., et al., *Adult human kidney organoids originate from CD24.* Nat Genet, 2022.
445 **54**(11): p. 1690-1701.
446 10. Mori, Y., et al., *KIM-1 mediates fatty acid uptake by renal tubular cells to promote*
447 *progressive diabetic kidney disease.* Cell Metab, 2021. **33**(5): p. 1042-1061 e7.
448 11. Latcha, S., et al., *Long-Term Renal Outcomes after Cisplatin Treatment.* Clin J Am Soc
449 Nephrol, 2016. **11**(7): p. 1173-1179.
450 12. McSweeney, K.R., et al., *Mechanisms of Cisplatin-Induced Acute Kidney Injury:*
451 *Pathological Mechanisms, Pharmacological Interventions, and Genetic Mitigations.*
452 Cancers (Basel), 2021. **13**(7).
453 13. Miller, R.P., et al., *Mechanisms of Cisplatin nephrotoxicity.* Toxins (Basel), 2010. **2**(11):
454 p. 2490-518.
455 14. Sato, Y., M. Takahashi, and M. Yanagita, *Pathophysiology of AKI to CKD progression.*
456 Semin Nephrol, 2020. **40**(2): p. 206-215.
457 15. Ferenbach, D.A. and J.V. Bonventre, *Mechanisms of maladaptive repair after AKI leading*
458 *to accelerated kidney ageing and CKD.* Nat Rev Nephrol, 2015. **11**(5): p. 264-76.
459 16. Nielsen, R., E.I. Christensen, and H. Birn, *Megalin and cubilin in proximal tubule protein*
460 *reabsorption: from experimental models to human disease.* Kidney Int, 2016. **89**(1): p. 58-
461 67.
462 17. Mody, H., et al., *Pharmacodynamic Modeling to Evaluate the Impact of Cimetidine, an*
463 *OCT2 Inhibitor, on the Anticancer Effects of Cisplatin.* Cells, 2022. **12**(1).
464 18. Kuo, L.J. and L.X. Yang, *Gamma-H2AX - a novel biomarker for DNA double-strand*
465 *breaks.* In Vivo, 2008. **22**(3): p. 305-9.
466 19. Han, W.K., et al., *Kidney Injury Molecule-1 (KIM-1): a novel biomarker for human renal*
467 *proximal tubule injury.* Kidney Int, 2002. **62**(1): p. 237-44.
468 20. Tang, C., et al., *Cisplatin nephrotoxicity: new insights and therapeutic implications.* Nat
469 Rev Nephrol, 2023. **19**(1): p. 53-72.
470 21. Lovisa, S., et al., *Epithelial-to-mesenchymal transition induces cell cycle arrest and*
471 *parenchymal damage in renal fibrosis.* Nat Med, 2015. **21**(9): p. 998-1009.

472 22. Grande, M.T., et al., *Snail1-induced partial epithelial-to-mesenchymal transition drives*
473 *renal fibrosis in mice and can be targeted to reverse established disease.* Nat Med, 2015.
474 **21**(9): p. 989-97.
475 23. Patteson, A.E., et al., *Vimentin protects cells against nuclear rupture and DNA damage*
476 *during migration.* J Cell Biol, 2019. **218**(12): p. 4079-4092.
477 24. Li, S., et al., *Tubular cell senescence promotes maladaptive kidney repair and chronic*
478 *kidney disease after cisplatin nephrotoxicity.* JCI Insight, 2023. **8**(8).
479 25. Liu, B.C., et al., *Renal tubule injury: a driving force toward chronic kidney disease.* Kidney
480 Int, 2018. **93**(3): p. 568-579.
481 26. LeBleu, V.S., et al., *Origin and function of myofibroblasts in kidney fibrosis.* Nat Med,
482 2013. **19**(8): p. 1047-53.
483 27. Gupta, N., et al., *Modeling injury and repair in kidney organoids reveals that homologous*
484 *recombination governs tubular intrinsic repair.* Sci Transl Med, 2022. **14**(634): p.
485 eabj4772.
486 28. Hiratsuka, K., et al., *Organoid-on-a-chip model of human ARPKD reveals mechanosensing*
487 *pathomechanisms for drug discovery.* Sci Adv, 2022. **8**(38): p. eabq0866.
488 29. Tabibzadeh, N., et al., *Navigating the kidney organoid: insights into assessment and*
489 *enhancement of nephron function.* Am J Physiol Renal Physiol, 2023. **325**(6): p. F695-
490 F706.
491 30. Yousef Yengej, F.A., et al., *Kidney Organoids and Tubuloids.* Cells, 2020. **9**(6).
492 31. Yousef Yengej, F.A., et al., *Tubuloid differentiation to model the human distal nephron*
493 *and collecting duct in health and disease.* Cell Rep, 2023. **43**(1): p. 113614.
494 32. Wiraja, C., et al., *Nephrotoxicity Assessment with Human Kidney Tubuloids using*
495 *Spherical Nucleic Acid-Based mRNA Nanoflares.* Nano Lett, 2021. **21**(13): p. 5850-5858.
496 33. Vidal Yucha, S.E., et al., *"3D, human renal proximal tubule (RPTEC-TERT1) organoids*
497 *'tubuloids' for translatable evaluation of nephrotoxins in high-throughput".* PLoS One,
498 2022. **17**(11): p. e0277937.
499 34. Yousef Yengej, F.A., et al., *Tubuloid differentiation to model the human distal nephron*
500 *and collecting duct in health and disease.* Cell Rep, 2024. **43**(1): p. 113614.
501 35. Fu, Y., et al., *Chronic effects of repeated low-dose cisplatin treatment in mouse kidneys*
502 *and renal tubular cells.* Am J Physiol Renal Physiol, 2019. **317**(6): p. F1582-F1592.
503 36. Gijzen, L., et al., *Culture and analysis of kidney tubuloids and perfused tubuloid cells-on-*
504 *a-chip.* Nat Protoc, 2021. **16**(4): p. 2023-2050.
505 37. Ichimura, T., et al., *Kidney injury molecule-1 is a phosphatidylserine receptor that confers*
506 *a phagocytic phenotype on epithelial cells.* J Clin Invest, 2008. **118**(5): p. 1657-68.
507 38. Cong, W., et al., *Implications of the Wnt5a/CaMKII pathway in retinoic acid-induced*
508 *myogenic tongue abnormalities of developing mice.* Sci Rep, 2014. **4**: p. 6082.
509 39. Takai, J., et al., *heterozygous mutant mice exhibit reduced inflammatory responses and*
510 *impaired bacterial clearance.* iScience, 2021. **24**(8): p. 102836.
511

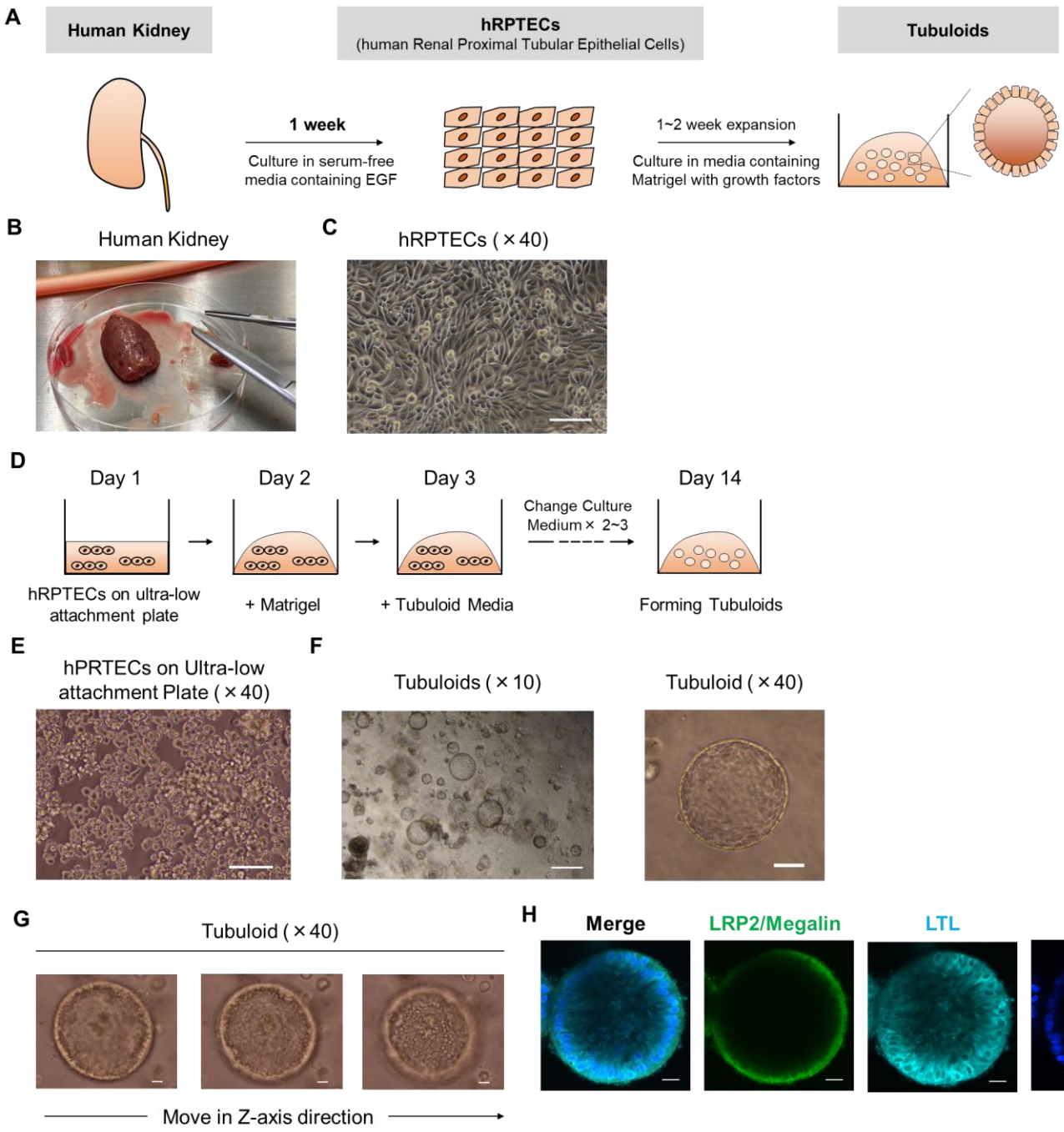
A
Human Kidney
hRPTECs
(human Renal Proximal Tubular Epithelial Cells)
Tubuloids
1 week
Culture in serum-free media containing EGF
1~2 week expansion
Culture in media containing Matrigel with growth factors
B
Human Kidney
C
hRPTECs (×40)
D
Day 1
Day 2
Day 3
Change Culture Medium × 2~3
Day 14
hRPTECs on ultra-low attachment plate
+ Matrigel
+ Tubuloid Media
Forming Tubuloids
E
hPRTECs on Ultra-low attachment Plate (×40)
F
Tubuloids (×10)
Tubuloid (×40)
G
Tubuloid (×40)
Move in Z-axis direction
H
Merge
LRP2/Megalin
LTL
DAPI

Figure 1

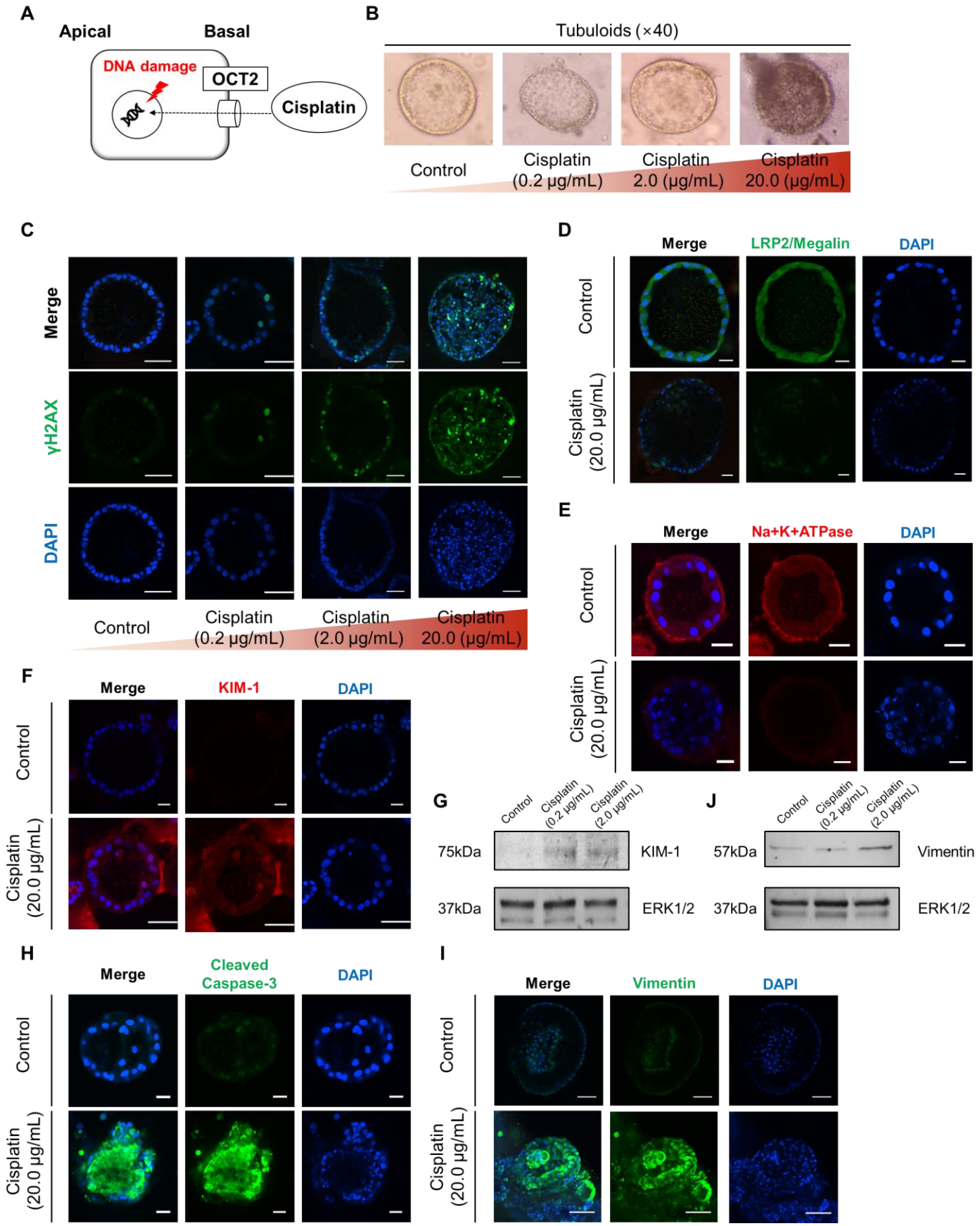
A
Apical
Basal
DNA damage
OCT2
Cisplatin
B
Tubuloids (×40)
Control
Cisplatin (0.2 μg/mL)
Cisplatin 2.0 (μg/mL)
Cisplatin 20.0 (μg/mL)
C
Merge
γH2AX
DAPI
Control
Cisplatin (0.2 μg/mL)
Cisplatin (2.0 μg/mL)
Cisplatin 20.0 (μg/mL)
D
Merge
LRP2/Megalin
DAPI
Control
Cisplatin (20.0 μg/mL)
E
Merge
Na+K+ATPase
DAPI
Control
Cisplatin (20.0 μg/mL)
F
Merge
KIM-1
DAPI
Control
Cisplatin (20.0 μg/mL)
G
Control
Cisplatin (0.2 μg/mL)
Cisplatin (2.0 μg/mL)
75kDa
KIM-1
37kDa
ERK1/2
J
Control
Cisplatin (0.2 μg/mL)
Cisplatin (2.0 μg/mL)
57kDa
Vimentin
37kDa
ERK1/2
H
Merge
Cleaved Caspase-3
DAPI
Control
Cisplatin (20.0 μg/mL)
I
Merge
Vimentin
DAPI
Control
Cisplatin (20.0 μg/mL)

Figure 2

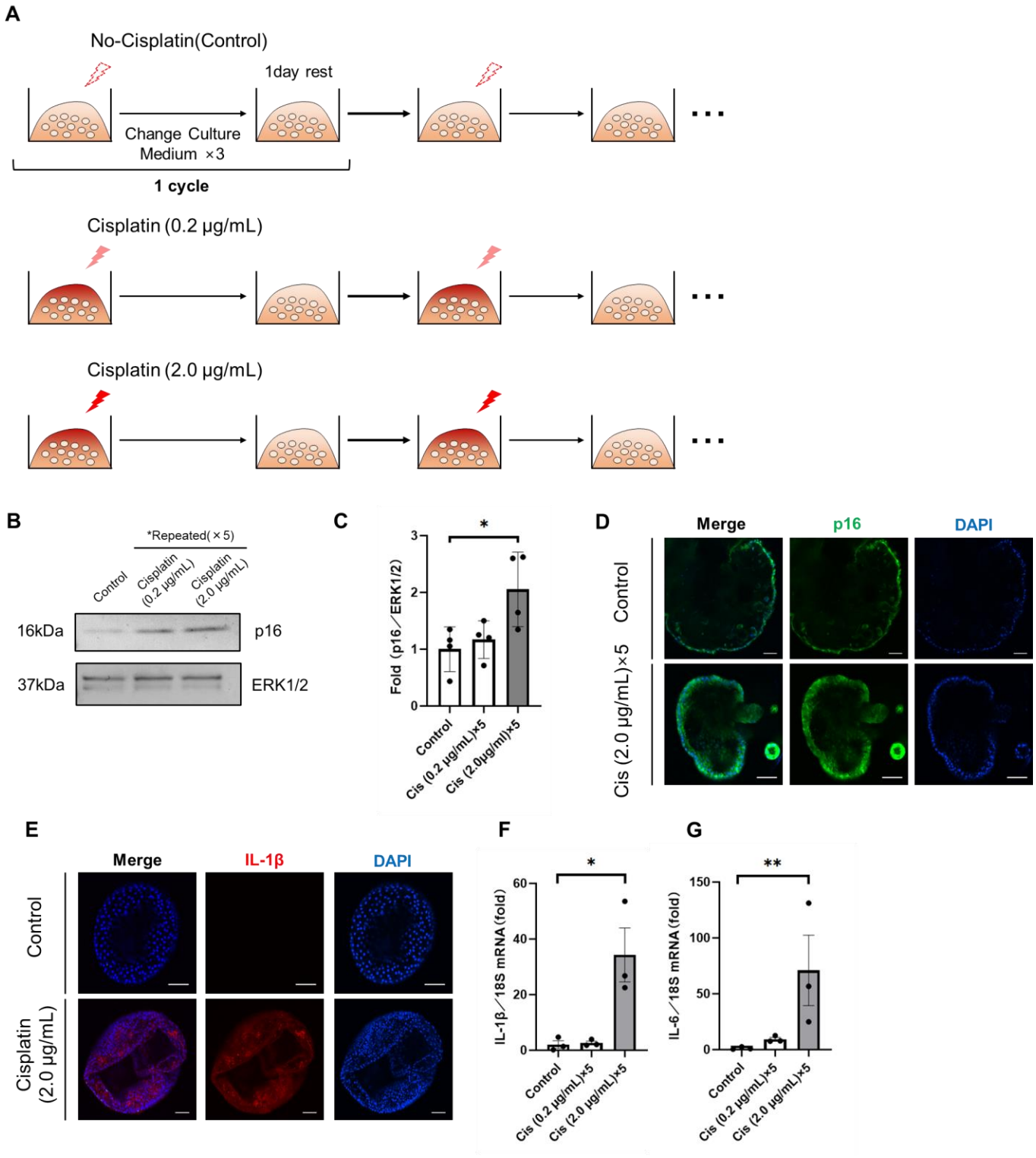
A
No-Cisplatin(Control)
1day rest
Change Culture Medium ×3
1 cycle
Cisplatin (0.2 μg/mL)
Cisplatin (2.0 μg/mL)
B
*Repeated(×5)
Control
Cisplatin (0.2 μg/mL)
Cisplatin (2.0 μg/mL)
16kDa
p16
37kDa
ERK1/2
C
Fold (p16／ERK1/2)
Control
Cis (0.2 μg/mL)×5
Cis (2.0μg/ml)×5
D
Merge
p16
DAPI
Control
Cis (2.0 μg/mL)×5
E
Merge
IL-1β
DAPI
Control
Cisplatin (2.0 μg/mL)
F
IL-1β／18S mRNA (fold)
G
IL-6／18S mRNA (fold)

Figure 3

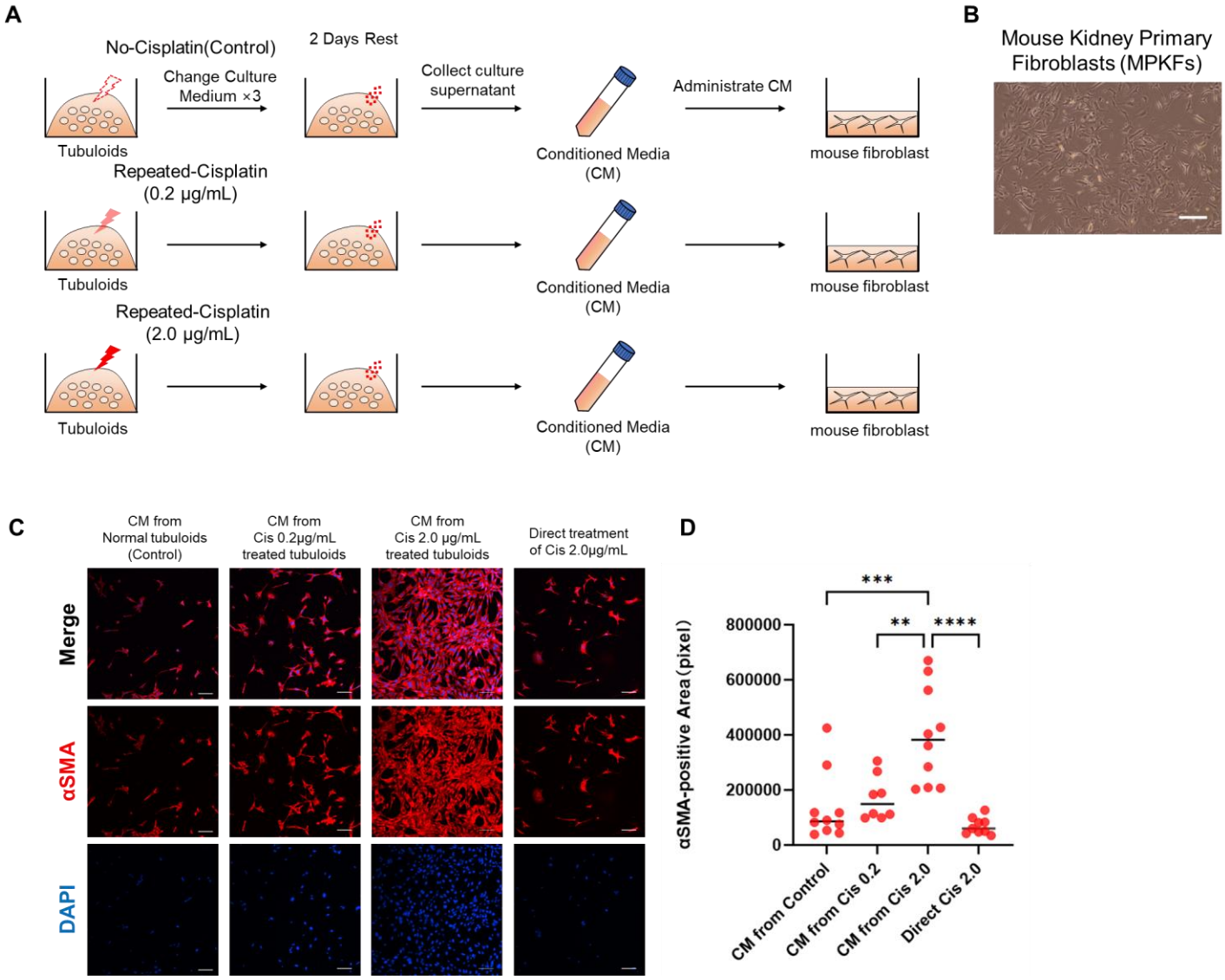
A
No-Cisplatin(Control)
Change Culture Medium ×3
2 Days Rest
Collect culture supernatant
Administrate CM
Tubuloids
Conditioned Media (CM)
mouse fibroblast
Repeated-Cisplatin (0.2 μg/mL)
Repeated-Cisplatin (2.0 μg/mL)
B
Mouse Kidney Primary Fibroblasts (MPKFs)
C
CM from Normal tubuloids (Control)
CM from Cis 0.2μg/mL treated tubuloids
CM from Cis 2.0 μg/mL treated tubuloids
Direct treatment of Cis 2.0μg/mL
Merge
αSMA
DAPI
D
αSMA-positive Area (pixel)
800000
600000
400000
200000
0
***
**
****
CM from Control
CM from Cis 0.2
CM from Cis 2.0
Direct Cis 2.0

Figure 4

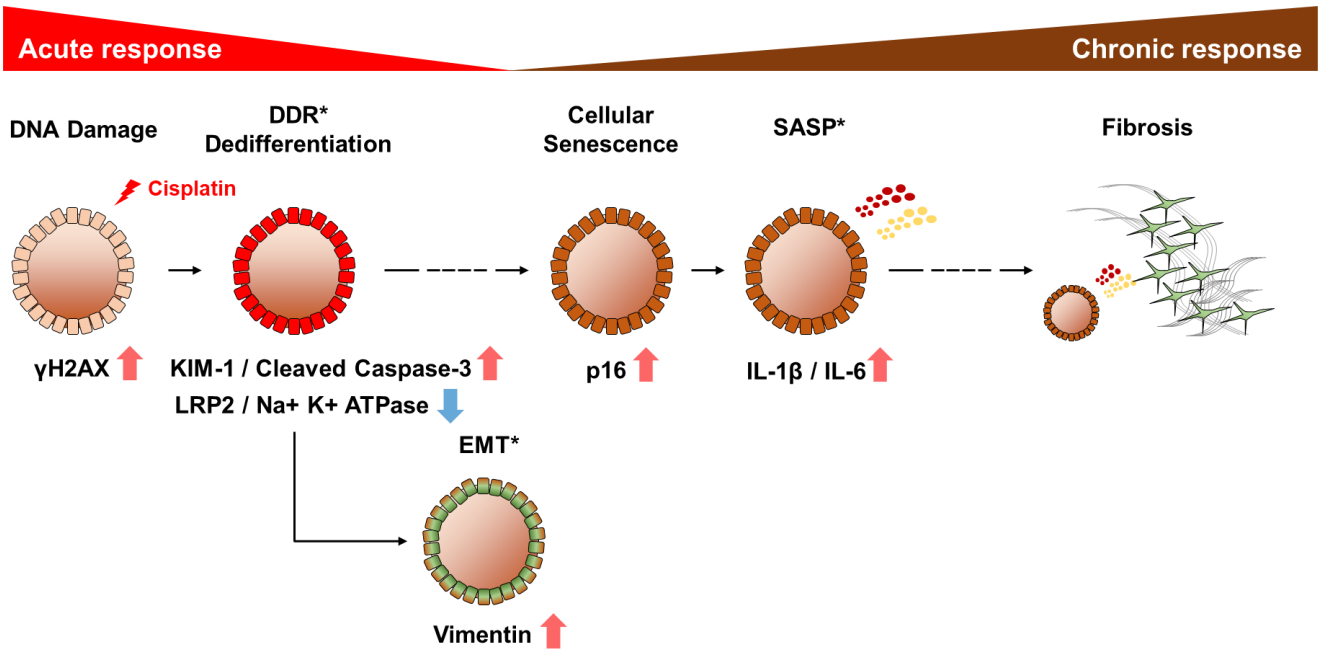

DDR: DNA Damage Response

SASP: Senescence Associated Secretary Phenotype

EMT: Epithelial-Mesenchymal Transition

Figure 5